

# Calculation of the Point-on-Wave for Voltage Dips in Three-Phase Systems

Ying Wang <sup>ID</sup>, Senior Member, IEEE, Ling-Feng Deng <sup>ID</sup>, Math H. J. Bollen <sup>ID</sup>, Fellow, IEEE,  
and Xian-Yong Xiao <sup>ID</sup>, Senior Member, IEEE

**Abstract**—Point-on-wave (POW) is a single-event characteristic of voltage dips, influencing the performance of sensitive equipment, such as AC contactor and wind turbines. However, definition and calculation of POW are unsolved issues. The existing definition of POW is for single-phase dips; it does not consider three-phase dips. Moreover, existing POW calculation methods are inaccurate. This paper proposes a definition of POW as a single-event characteristic for three-phase voltage dips. Then, it proposes a POW calculation method based on space vector, including POW detection and angle calculation. The proposed method is based on the ellipse characteristics during the dip-stage and non-dip stage. The proposed method does not depend on zero crossing for angle reference. To verify the performance of the proposed method, a power-system simulation model is built to generate voltage dips with different origin. Furthermore, the accuracy of the proposed method is verified by 425 sets measured voltage dips, and compared with the published methods.

**Index Terms**—Power quality, voltage dip, point-on-wave, space vector, angle calculation method.

## I. INTRODUCTION

IN THE field of voltage dip detection and characteristics calculation [1]–[5], residual voltage and duration are the main characteristics of voltage dips and used to assess the performance of sensitive equipment. Extensive tests have shown that point-on-wave (POW), another important single-event characteristic, effects the performance of sensitive equipment, such as AC contactor (ACC), low-voltage release (LVR) [6]–[11], and wind turbines [12], [13]. However, POW calculation and some related issues remain unsolved [14].

Unsolved issues of POW include three things. The first one is the definition of POW for three-phase voltage dips. POW is defined as “the phase angle at which a voltage dip begins” by IEC [2] and as “the phase angle where disturbance waveform deviates from the reference waveform by 10% and 5%” by IEEE [15]. However, there is no definition and calculation method for three-phase dips. This is among the need of three-phase equipment,

Manuscript received June 14, 2019; revised October 4, 2019 and December 3, 2019; accepted December 14, 2019. Date of publication December 18, 2019; date of current version July 23, 2020. This work was supported by the National Natural Science Foundation of China under Grant 51807126. Paper no. TPWRD-00648-2019. (Corresponding author: Xian-Yong Xiao.)

Y. Wang, L.-F. Deng, and X.-Y. Xiao are with the College of Electrical Engineering, Sichuan University, Chengdu 610017, China (e-mail: tuantuan1125@qq.com; 983969291@qq.com; xiaoxianyong@163.com).

M. H. J. Bollen is with the Luleå University of Technology, 93187 Skellefteå, Sweden (e-mail: math.bollen@ltu.se).

Color versions of one or more of the figures in this article are available online at <http://ieeexplore.ieee.org>.

Digital Object Identifier 10.1109/TPWRD.2019.2960524

like wind turbines, which are sensitive to POW [12], [13]. When detecting a dip, POWs of the three phases differ by 120°. It is unsolved which one of the three angles represents the single-event characteristic. Moreover, slowly recovering dips, do not have a POW of recovery (POW-R), but most algorithms do result in a value, albeit unrealistic, of POW-R. A clear definition is needed here.

The second issue concerns the detection of POW. Existing methods can be divided into, rms voltage-based method [16], [17], voltage waveform-based method [15] and time-frequency transform-based method [18]–[22]. The main rms voltage-based methods, calculate POW according to the instant when a threshold (90% or 95%) of the rms voltage is exceeded [16]. This is referred to as rms voltage threshold method (RVT) in this paper. There is no link between the threshold of 0.9 p.u. and the two POWs, as will be explained in Section II.A. Reference [17] proposes a method to determine the inception and the recovery instant of dip, by calculating the absolute rms voltage difference between two adjacent sliding windows, referred to as rms voltage difference method (RVD) in this paper. This method often gives the correct POW. However, instantaneous time, phase and polarity information are lost by calculating rms voltage, which may lead to inaccurate detection of POW. Among voltage waveform-based methods, [15] presents a waveform envelope approach, but it is hard to obtain an accurate reference waveform in practice. Among time-frequency transform-based methods, wavelet transform method is most widely used [18]–[22]. However, the calculation process is complex and vulnerable to noise.

The third issue concerns the calculation of the angle of POW. When quantifying or calculating this angle, a reference point is needed. “The upward zero crossing of the fundamental voltage” is used in [8], [23]. Several factors influence the accuracy of the angle calculation method, for example, the number of sampling points in one cycle.

Due to their effect on sensitive equipment [6]–[13], a definition and methods for calculation of POW are needed. Extensive tests and simulations on sensitive equipment, show different performance for different POW (with the same residual voltage and duration). In China, POW is considered for inclusion in a national recommended practice for testing sensitive equipment under voltage dips.

This paper presents a mathematical method to define POW as a single-event characteristic of three-phase voltage dips, including rectangular dips, slowly recovering dips and multistage dips. Moreover, this paper proposes a method to calculate POW based

on space vector, including detection of initiation and recovery points and calculation of the angle directly, not depending on the upward zero-crossing point reference. The contributions of this paper are towards solving the three issues mentioned above.

The structure of this paper is as follows. The definition of POW for three-phase voltage dips, including rectangular, slowly recovering and multistage dips, is proposed in Section II. Section III proposes a method to calculate POW of dip initiation and POW of dip recovery by using the space vector, including detection of initiation and recovery points and calculation of POW angle. Section IV verifies the performance of the proposed method using simulated dips. Section V uses 425 measured dips to verify the accuracy of the proposed method. Extensive comparisons between the proposed and other published methods are shown. The conclusions are presented in Section VI.

## II. THE DEFINITION OF POW

### A. Three POW Values

Three POW values are presented in this paper, including “real POW”, “visual inspection value of POW” and “estimated value of POW”, which are defined as follows.

- Real POW. It is the actual phase angle of the fundamental voltage waveform at which the voltage dip starts or ends. The real POW of a measured voltage dip is unknown. For a simulated voltage dip, the real POW is set by the simulation parameters.
- Visual inspection value (Visual value) of POW. As there is no direct information on the real POW for a measured voltage dip, this paper gets the visual inspection value of POW manually. In many cases, the visual inspection POW is close to the real POW. For simulated voltage dips, whose real POW is known, there is no need to get the visual inspection POW.
- Estimated value of POW. It is the POW calculated by the proposed method or any other published method.

The estimated POW is compared with the real POW for simulated dip, or with the visual value for measured dips, to verify the performance of the methods.

### B. Definition of POW for Single-Phase Voltage Dips

Corresponding to fault “starting” and “ending”, “point-on-wave of dip initiation (POW-I)” and “point-on-wave of dip recovery (POW-R)” are two single-event indices. POW-I is the phase angle of the fundamental voltage waveform at which the voltage dip starts. POW-R is the phase angle of the fundamental voltage waveform at which the main recovery takes place [17], [23]. Two examples will be used to show POW and to explain the errors made by the RVT method.

The real POW is the phase angle of the fundamental voltage waveform when the fault starts or ends. Fig. 1(a) and (b) show a measurement example (Example 1) to illustrate the POW-I. The threshold (0.9 p.u.) of the rms voltage is indicated as a black dotted line in (a), at 416.5 V. The waveform of this dip is plotted in blue in (b). Choosing 0.9 p.u. as threshold (RVT method), the POW-I takes place at 4.75 cycles in (b), indicated as a black

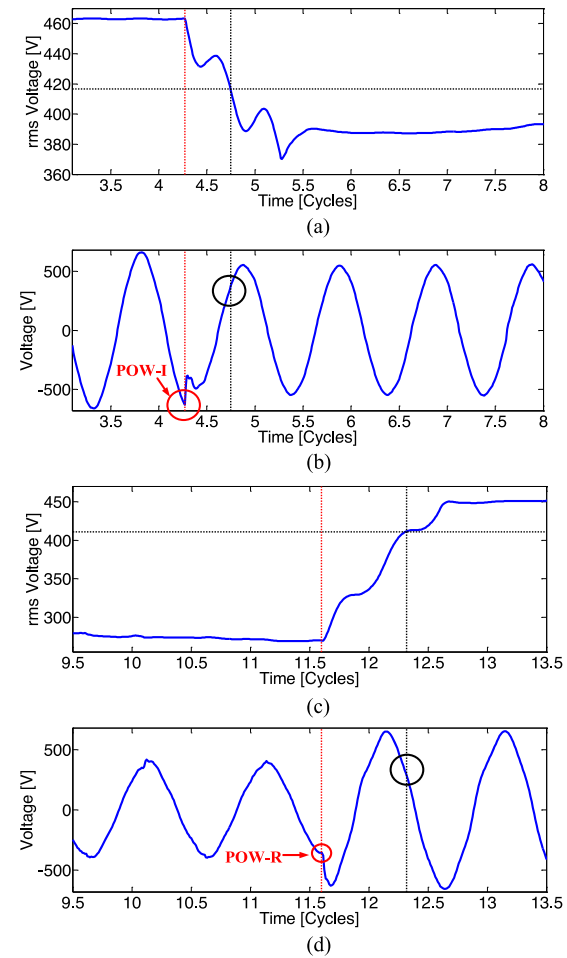


Fig. 1. Two examples are to show the real POW. (a) The rms voltage of Example 1. (b) The voltage waveform of Example 1. (c) The rms voltage of Example 2. (d) The voltage waveform of Example 2.

circle, while the real POW-I is at 4.3 cycles, indicated by the red circle in (b). The red dotted lines indicate fault starting, in (a) and (b). At the fault starting point, corresponding to POW-I, the rms voltage deviates from the nominal voltage in (a), and the waveform shows an obvious change in (b).

Another recorded waveform (Example 2) is shown in (c) and (d) to illustrate the POW-R. The rms voltage is shown in (c). The threshold (0.9 p.u., 410.8 V) is indicated as a black dotted line. The POW-R by RVT method is at 12.32 cycles, black circle in (d); the real POW-R is at 11.6 cycles, red circle in (d). For the fault clearing point, corresponding to POW-R, the rms voltage and the recorded waveform show obvious deviation in (c) and (d).

Thus, using the RVT method will not give an accurate estimation of the real POW [17], [24].

### C. Definition of POW for Three-Phase Voltage Dips

The definition of POW as given above, can be used for single-phase voltage dips. However, no definition and calculation method exist of POW for three-phase voltage dips. The POWs of the three phases are different, with  $120^\circ$  between neighboring phases.

This paper proposes a definition of POW for three phase voltage dips, as a single-event characteristic, based on the symmetry of voltage dips.

- Balanced voltage dip: POW as a single-event characteristic is the POW of phase a.
- Unbalanced voltage dip: POW as a single-event characteristic is the POW of the phase-to-neutral voltage with the lowest residual voltage.

For a measured voltage dip, it is known on which phase has the lowest residual voltage. The POW calculated method could be used to calculate POW for this phase to obtain the single-event characteristic of the dip.

There are various algorithms to distinguish between balanced and unbalanced voltage dip, which is not the scope of this paper. In this paper, the algorithm proposed in [25] is used to determine whether a voltage dip is a balanced dip.

Combining POW of phase a and the dip type, POW as a single-event characteristic can be calculated.

#### D. Slowly Recovering Voltage Dip

A short circuit fault, results in a rectangular voltage dip, due to the actions of protection equipment. Transformer energizing and motor starting result in slowly recovering voltage dips, which do not have any real POW-R. Both switching actions result in a slowly recovering voltage dip. When a motor connected to the power system, a large inrush current is drawn, so a voltage dip is produced. The inrush current produces a torque, which makes the motor to spin. Once the spin starts, a counter voltage is induced in the rotor winding. This voltage opposes the flow of the current (Lenz's law), and the inrush current starts to reduce. The counter voltage is in proportion to the motor speed. When the motor reaches its rated speed, the counter voltage approaches rated voltage of the motor. Thus, the residual voltage of the dip recoveries slowly with the increase of rotational speed. It is a slow process, not a step change. It is similar that the voltage recovery of transformer energizing, the detailed is not elaborated here due to the limit space.

Based on the analysis mentioned above, although a value for POW-R can be obtained by most of the published algorithms, the slowly recovering voltage dip does not have a real POW-R. Before calculating POW, the voltage dip should be classified, and the right POW could be obtained based on the category of voltage dips. Reference [26] proposes a method with high accuracy for automatic classification of power quality events by using rms voltage, which is used to identify slowly recovering voltage dips in this paper.

#### E. Multistage Voltage Dip

Multistage dips are due to faults. They present different levels of magnitude before voltage returns back to normal. These different dip stages are due to changes in system configuration while the protection system isolate the fault or due to changes in the fault [27].

Characterization of multistage voltage dips has not been standardized and is not well defined. IEEE 1564 defines the residual voltage as the minimum of rms voltage recorded during a voltage

dip. It discusses the duration of multiple events in Annex B, including multistage dips and time aggregation of successive individual dips [16]. IEC 61000-4-30 defines the residual voltage is the lowest rms voltage measured on any channel during the dip; there is no mentioning of multistage voltage dips [2].

The effect of multistage voltage dips on sensitive equipment is studied in [10], where tests on AC coil contactors under various two-stage voltage dips are presented. The performances of contactor are different under dips with the same two stages but different stage order. However, there is no clear study after the performance of sensitive equipment under POWs of different stages, nor any related definition in any standard for POWs of the different stages. That is an important subject in future to explore, but is not included in this paper.

The number of POW points for multistage voltage dip varies between dips. It depends on the evolution of the fault, the instants of breaker opening on two sides of the line, and so on. For example, consider that a fault starts as single-line-to-ground, evolves to three-phase-to-ground, and is cleared by a single protection device; This would result in a dip with two POW-Is but only one POW-R. When a two-phase-to-ground or three-phase-fault is cleared at two or three different instants, the multistage voltage dip has one POW-I and two or three POW-Rs. It is difficult to determine the number of POWs only by the recorded waveform. The detailed information is need, including the information about relay action and the fault from the utility.

Due to lack of the knowledge as follow: 1) the performances of sensitive equipment under POWs of different stages; 2) the information of relay action and the fault, only one POW-I and one POW-R for the multistage dip are detected and calculated in this paper. The former is the first POW-I of the event, and the latter is last POW-R of the event. That is, the POW-I and POW-R are the phase angle at the initial occurrence moment of the fault and the final clearance moment of the fault, respectively.

### III. THE PROPOSED CALCULATION METHOD

Based on the space vector in a three-phase system, this section presents a way of defining POW for a three-phase voltage dip, a method of directly calculating the angle of POW and a method of detecting the initiation point and recovery points, which are the major contributions of the paper.

#### A. Space Vector

Build a space vector by the waveform of  $v_a$ ,  $v_b$  and  $v_c$ :

$$x(t) = 2/3[v_a(t) + \alpha v_b(t) + \alpha^2 v_c(t)] \quad (1)$$

where  $\alpha = e^{j2\pi/3}$ . This space vector  $x(t)$  can be described as “the sum of positive ( $x_p$ ) and negative ( $x_n$ ) angular frequency phasors” [25], [28].

$$\vec{x} = x_p e^{j\omega t} + x_n e^{-j\omega t} \quad (2)$$

#### B. Defining POW Based on Space Vector

To define POW, the first thing is to define the initiation and recovery point of the voltage dip. Reference [29], [30] defines POW-I as “the angle in which the circle begins to deviate from

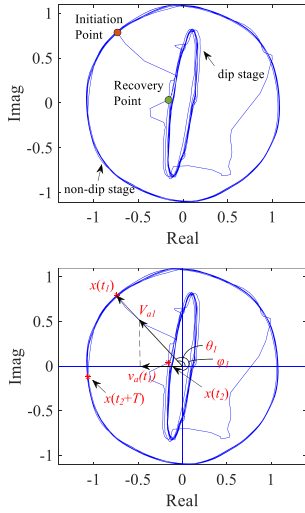


Fig. 2. The definition of POW. (a) The initiation and recovery points for Example 3. (b) The angle of POW for Example 3.

its normal trajectory and turn into an ellipse" and POW-R as "the angle in which the during fault ellipse begins to deviate from its trajectory and turn into a circle". However, no method to calculate POW for measured voltage dips is presented in [29], [30].

The vector  $\vec{x}$  is changing every sample. As shown in Fig. 2(a), the trajectory of  $\vec{x}$  in the complex plane is a circle when  $x_n = 0$ , which corresponds to the non-dip stage; and an ellipse when  $x_n \neq 0$ , which corresponds to the dip stage. During the non-dip stage, the space vector contains only positive angular frequency phasor, and the corresponding space vector follows a circle in the complex plane. During the dip stage for an unbalanced dip, the space vector contains positive and negative angular frequency phasors; the corresponding space vector follows an ellipse in the complex plane. For balanced dip,  $x_n = 0$  and the trajectory of space vector is a smaller circle [25], [29], [30].

This paper defines the initiation point as the point where the trajectory of  $\vec{x}$  begins to deviate from the no-dip circle to the ellipse or smaller circle. Similarly, the recovery point is defined as the point where the trajectory of  $\vec{x}$  starts to move from the ellipse or smaller circle to the no-dip circle.

For balanced three-phase voltages, the direction of the vectors  $V_a$ ,  $\alpha V_b$  and  $\alpha^2 V_c$  is the same, so  $\vec{x}$  keeps the direction of  $V_a$  when the trajectory is a circle. POW is the phase angle of the fundamental voltage waveform at the initiation or recovery point, thus it is possible to get the phase angle according to the angle of  $x(t)$  in the complex plane.

Considering Fig. 2(b), for POW-I, the space vector at the initiation point is denoted as  $x(t_1)$ . The angle of  $x(t_1)$  is the angle between the space vector and the real axis.

$$\theta_1 = \text{angle}(x(t_1)) \quad (3)$$

Because  $x(t)$  has the same direction as  $V_a$ ,  $\theta_1$  is also the angle between  $V_a(t_1)$  and the real axis. The relationship between instantaneous value of  $v_a$  and  $\theta$  is as follows:

$$v_a(t_1) = V_{am} * \cos\theta_1 \quad (4)$$

where  $V_{am}$  is the peak amplitude of  $V_a$ .

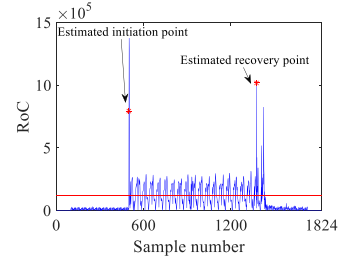


Fig. 3. To find the initiation point and recovery point by RoC for Example 3.

POW is the phase angle referred to the last upward zero crossing of the pre-dip voltage; using a sine function to describe  $v_a$  and to get POW  $\varphi_1$ :

$$v_a(t_1) = V_{am} * \sin\varphi_1 = V_{am} * \cos(\varphi_1 - \pi/2) \quad (5)$$

Combining (4) and (5), POW-I gives:

$$\text{POW} - I = \varphi_1 = \theta_1 + \pi/2 \quad (6)$$

A similar method can be used to calculate POW-R. Note that  $x(t)$  at the recovery point has not yet returned to the circular trajectory, that is  $x(t_2)$  in Fig. 2(b). The three-phase voltage is not balanced at  $t_2$ , so  $x(t_2)$  and  $V_a(t_2)$  may not have the same direction. However,  $x(t_2 + T)$  returns to the circle ( $T$  is one cycle),  $V_a(t_2 + T)$  has the same direction of  $V_a(t_2)$ . The phase angle of the fundamental voltage waveform at the recovery point is  $\varphi(t_2) = \varphi(t_2 + T)$ . Making  $\theta_2 = \text{angle}(x(t_2 + T))$  and substituting in (5) and (6) to get POW-R:

$$\text{POW} - R = \varphi(t_2) = \varphi(t_2 + T) = \theta_2 + \pi/2 \quad (7)$$

### C. Definition of Detection Index

The absolute value of  $x(t)$  is the distance to the origin, denoted as  $r(i)$  for the sample point  $i$ . This paper introduces the rate of change ( $RoC$ ) for the distance to the origin as a characteristic versus time:

$$RoC(i) = \frac{|r(i) - r(i+1)|}{\Delta t} \quad (8)$$

The absolute value of the difference between  $r(i)$  and  $r(i+1)$  shows the variation from point to point. The absolute value is divided by the sample step  $\Delta t$ , resulting in the time derivative (rate-of-change) of the distance to the origin.

### D. Detecting Initiation Point

The initiation point is the point of voltage dip starting; the point where the radius of the space vector begins to change.  $RoC$  will suddenly increase at the initiation point. Choose  $p * r(1)$  as the threshold for detecting initiation point. The dimension of  $p$  is p.u./s,  $r(1)$  is the first sample's distance to the origin for a recorded waveform, which is assumed to be in normal operation. Compare  $RoC$  with the threshold, the first point whose  $RoC$  exceeds the threshold is the initiation point, as shown in Fig. 3. In Fig. 3, the x-axis is the sample number for Example 3, y-axis is  $RoC$ , the red line is the threshold, and the blue line is  $RoC$  versus time.

TABLE I  
STANDARD DEVIATION OF RESULTS WITH DIFFERENT THRESHOLD

$p$ [p.u./s]	60	70	80	90	100
$SD$	67.1	54.6	45.9	43.9	40.9
$p$ [p.u./s]	110	120	130	140	150
$SD$	39.7	41.0	43.8	41.2	44.8

The standard deviation is the smallest when  $p = 110$  p.u./s in Table I, so choose  $p = 110$  p.u./s for this algorithm, based on the calculation of measured voltage dips.

The key to detecting POW-I accurately, is to choose a suitable  $p$ . There were 425 measured voltage dips used for this paper, containing dips of different types. Detailed information is given in Section V.A. The POWs were calculated for these 425 measured dips, choosing  $p$  from 60 to 150, in steps of 10. Ten sets of POW results by different  $p$  are compared with the Visual value. The standard deviations of the difference for different thresholds are shown in Table I. The expression for calculating standard deviation is as follows:

$$SD_p = \sqrt{\frac{1}{N} \sum_{i=1}^N (\varphi_{pi} - \varphi_{Vi})^2} \quad (9)$$

In (9),  $N$  is the total number of measured dips,  $SD_p$  is the standard deviation between the calculated result when the threshold is  $p$  and the Visual value,  $\varphi_{pi}$  is the POW-I of the  $i^{\text{th}}$  measured dip by the proposed method, when the threshold is  $p$ , and  $\varphi_{Vi}$  is Visual value for this dip.

The standard deviation is a measure of the dispersion between the estimated results and the Visual value. The greater the standard deviation, the greater the difference between the estimated results and Visual values (which are close to the real POW). According to this property, the optimal  $p$  could be selected to detect POW-I.

#### E. Detecting Recovery Point

The recovery point is the point where the main recovery takes place; the point that moves from ellipse or smaller circle to the non-dip circle. Theoretically, the radius of the space vector at that point will show a more obvious change than that of the ellipse trajectory. Therefore, the recovery point should be the maximum  $RoC$  in the recovery segment (the second transition segment); the recovery point estimated by the proposed method is the point with greatest  $RoC$  in the second transition segment. For a multistage voltage dip, the estimated recovery point is the point with highest  $RoC$  in the last transition segment, as shown in Fig. 3. The method of finding the point with highest  $RoC$  in the second transition segment is introduced in [15]. The algorithm is briefly explained as follows.

- 1) Use the traditional rms voltage threshold method (RVT method) to estimate approximately the position  $k_{rec0}$  of the recovery points.
- 2) The detected point by RVT method has a delay about one cycle in determining the recovery point. Therefore, traverse  $RoC$  from  $k_{rec0}$  to  $k_{rec0} - N$  ( $N$  is the number of

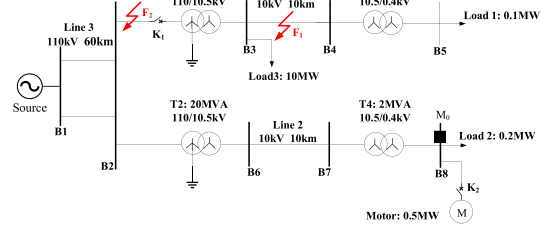


Fig. 4. Simulation model to generate voltage dips.

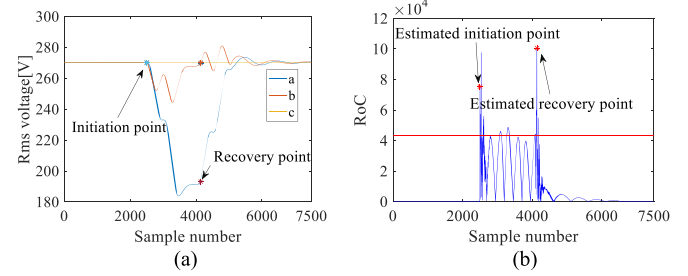


Fig. 5. A voltage dip caused by short-circuit fault. (a) The rms voltage waveform. (b) The  $RoC$  by the proposed method.

sampling points per cycle), and select the point with the highest  $RoC$  as the estimated recovery point.

#### IV. COMPARISON AND ANALYSIS FOR SIMULATED DIPS

To verify the performance of the proposed method, this section builds a simulation model of the power system generating dips due to short-circuit faults, motor starting, transformer energizing, simultaneous faults, and developing faults. Background harmonic and noise are considered in the model. The performance of the proposed method is verified using the data generated from this model.

##### A. The Data of the Simulation Model

A power system simulation model (with voltage levels of 110/10.5/0.38 kV and frequency of 50 Hz) built in Matlab/Simulink, is shown in Fig. 4. The model contains a voltage source of 110 kV, 8 buses (B1-B8), 2 Loads (Load 1 and Load 2) and 4 transformers (the connection type of T1 and T2 are Yn/Y, T3 and T4 are Y/Y). A motor is connected to B8. A monitor  $M_0$  is connected to B8 to record the voltage dip waveforms.  $F_1$  is a short-circuit fault occurring at Line 1. The location of  $F_1$  is 3 km to B3.  $F_2$  is a short-circuit fault close to B2.

The different situations are selected to get different voltage dip waveforms, with a sampling rate of 1000 points/cycle.

##### B. Voltage Dip Due to Short-Circuit Fault

Fault is the most common cause of voltage dip in power systems.  $F_1$  is a phase-to-phase to ground fault (Phase A and B), occurring at 0.05s, and cleared at 0.082s. The voltage dip waveform is shown in Fig. 5(a). According to the set fault starting and clearing time, initiation and recovery occur at samples 2501 and 4101, respectively. The  $RoC$  by the proposed method is

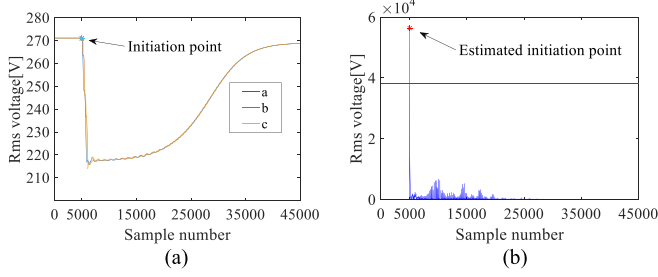


Fig. 6. Voltage dip caused by motor starting. (a) RMS voltage waveform. (b)  $RoC$  by the proposed method.

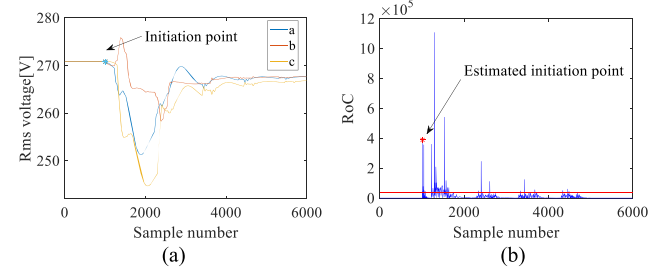


Fig. 7. Voltage dip caused by transformer energizing. (a) Rms voltage waveform. (b)  $RoC$  by the proposed method.

shown in Fig. 5(b). The estimated initiation point and recovery point are 2500 and 4101, respectively. Only the detection of the initiation point has the error of one point, which is a tiny error.

### C. Voltage Dip Due to Motor Starting

The large current generated by the starting of motor is also a common cause of voltage dips in a power system. A voltage dip is generated due to the motor starting in this section. Switch  $K_2$  is closed at 0.1 s, starting the motor.

A slowly recovering dip, with initiation point at 5001, is shown in Fig. 6(a). The performance of the proposed method is shown in Fig. 6(b). The estimated initiation point is 5001, in agreement with the real initiation point.

### D. Voltage Dip Due to Transformer Energizing

Breaker  $K_1$  closes at 0.02 s, resulting in transformer energizing and a slowly recovering dip. The initiation point corresponds to sample 1001, as shown in Fig. 7(a).

The performance of the proposed method is shown in Fig. 7(b). The estimated initiation point is 1001, again in agreement with the real value.

### E. Voltage Dip Due to Simultaneous Faults

It sometimes happens that the voltage dip occurs due to simultaneous faults, for example a trip caused by lightning. It has been simulated that  $F_1$  and  $F_2$  occur simultaneously, where  $F_1$  is a phase-to-phase to ground fault (Phase A and B), and  $F_2$  is a single-phase to ground fault (Phase C). The two faults are present from 0.05 s to 0.082 s. The rms voltage of this voltage dip is shown in Fig. 8(a), with the initiation at sample 2501 and recovery at sample 4101.

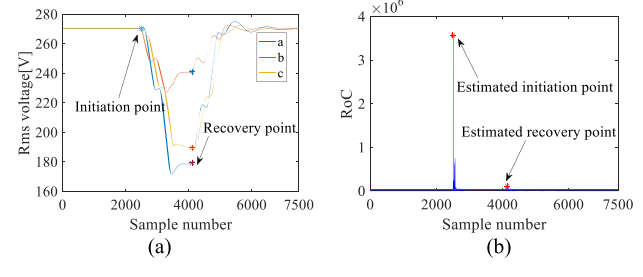


Fig. 8. Voltage dip caused by simultaneous faults. (a) RMS voltage waveform. (b)  $RoC$  by the proposed method.

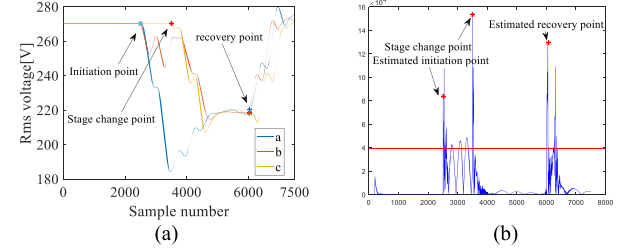


Fig. 9. Two-stage voltage dip caused by a developing fault. (a) RMS voltage waveform. (b)  $RoC$  by the proposed method.

For this dip,  $RoC$  is obvious for detecting the two points, because of the two faults starting at the same time, effecting the voltage more seriously. The estimated initiation and the recovery point are 2501 and 6001, in agreement with the real value. The proposed method shows a good performance for detecting POWs of dips due to simultaneous faults.

### F. Multistage Voltage Dip

A multistage voltage dip may be due to either a change of power system configuration while the protection system isolates a fault or due to changes in the fault. The latter is simulated in this section to generate a multistage voltage dip. At 0.05 s, a phase-to-phase to ground fault  $F_1$  (Phase A and B) occurs, and the fault develops into a three-phase short circuit fault at 0.07 s. The fault is cleared at 0.12 s. The resulting multistage voltage dip is shown in Fig. 9(a). The initiation point is the first initiation point of this event, which is sample 2501. The recovery point is the last recovery point of this event: sample 6001. The  $RoC$  is shown in Fig. 9(b), and the estimated points are 2501 and 6001, with the same as the real values.

This two-stage dip has a “stage change point”, representing the development of the event. In this case, the stage change point is at sample 3501. According to the analysis in Section II.E of this paper, the proposed method does not detect this point. However, as shown in Fig. 9(b), the proposed method can be improved to also detect this point.

### G. Voltage Dips Containing Harmonics and Noise

The performance of the proposed method may be influenced by harmonics and noise. This section generates voltage dips containing harmonics and noise, to explore their influence on the performance of the proposed method.

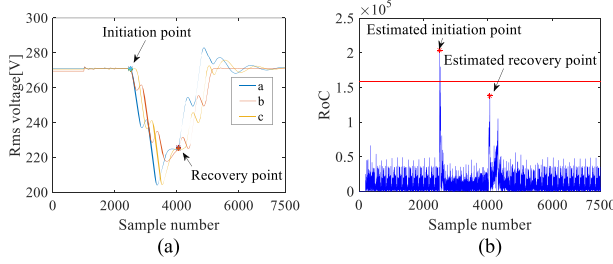


Fig. 10. Voltage dip caused by short-circuit fault with the background harmonic. (a) RMS voltage waveform. (b)  $RoC$  by the proposed method.

TABLE II  
THE PERFORMANCE OF SV METHOD INFLUENCED BY NOISE

SNR(dB)	Initiation point		Recovery point	
	Real	Estimated	Real	Estimated
10	2501	216	4101	4102
15	2501	2500	4101	4101
20	2501	2500	4101	4104
25	2501	2500	4101	4101
30	2501	2500	4101	4101

It is well known that non-linear loads in the power system lead to harmonic emission, especially power electronics devices, which are widely used in the power system. Load 2 is replaced with a non-linear load, and a three-phase fault occurs at  $F_1$ . A rectangular voltage dip containing harmonics is monitored by  $M_0$ , whose initiation point and recovery point are sample 2501 and 4101, respectively, as shown in Fig. 10(a). According to the FFT function of powergui block in Simulink, the voltage total harmonic distortion (THD) is 8.41%. For buses below 1 kV, the limit of THD is 8% in IEEE 519 [31]. Therefore, it is sufficient to use this simulation dip to analyze the influence of harmonics on the proposed method. The  $RoC$  is shown in Fig. 10(b), and the estimated initiation/recovery point is sample 2501/4101. Fig. 10(b) shows that the harmonic has an effect on the  $RoC$ , where the  $RoC$  in the non-dip stage is greater than without harmonic emission. However, there is only a small error in the detection of the recovery point (two samples difference corresponds to  $0.72^\circ$ ), indicating that the proposed method shows a good performance for detecting POW in power systems with large harmonic voltage distortion.

In addition, the noise in a real power system is inevitable. Since the voltage waveform, generated by the simulation model, did not contain any noise, Gaussian white noise has been added resulting in a Signal to Noise Ratio (SNR) of 10 to 40 dB (the step is 5 dB) for the rectangular voltage dip obtained in Section IV.B. The Gaussian white noise is generated by AWGN function in MATLAB. The performance of the proposed method is listed in Table II. The proposed method can detect accurately when the SNR is more than 15 dB. For dips with SNR lower than 10 dB, the proposed method gives an incorrect result.

## V. COMPARISON AND ANALYSIS FOR MEASURED DIPS

The 425 sets of measured voltage dips mentioned in Section III.D are used to verify the proposed and existing methods.

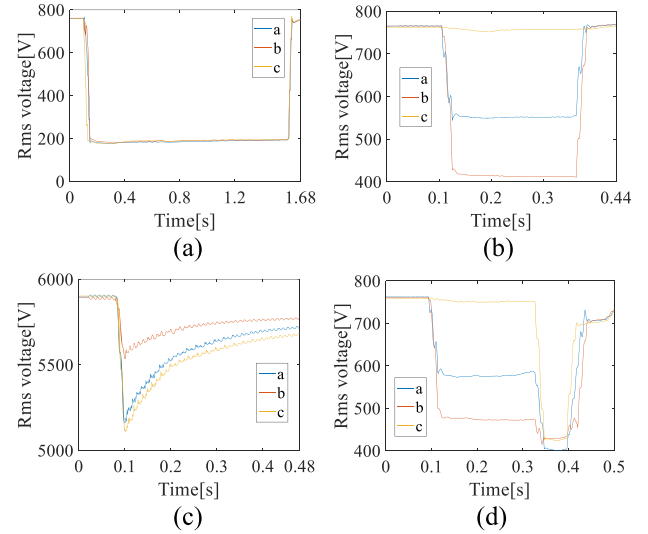


Fig. 11. Example of measured dips. (a) Balanced voltage dip. (b) Unbalanced rectangular voltage dip. (c) Slowly recovering voltage dip. (d) Multistage voltage dip.

The estimated results of each method are compared with Visual value for these 425 sets of measured voltage dips.

### A. The Measured Voltage Dips

The 425 measured voltage dips used in this paper include 353 rectangular dips and 72 slowly recovering dips. Among them, 149 rectangular dips and 14 slowly recovering dip are obtained from Göteborg Energi and Scottish Power; 204 rectangular dips and 58 slowly recovering dips are obtained from State grid electric power research institute of Henan Electric power company. There are 423 sets of unbalanced dips, accounting for 99.5% of the total. All dips are recorded at MV voltage level and the data set includes all typical types of dip. Four examples are shown in Fig. 11, to show the typical rms voltage waveform for four types of dips.

### B. Results by SV Method & Visual Value

A comparison between the results by SV method and Visual value, is shown in Fig. 12.(a) shows the 425 values of POW-I and (b) the 353 values of POW-R. The x-axis is Visual value, and y-axis is the result by SV method, when  $p = 110$  p.u./s. The blue scatters close to the red diagonal line means that the results by the two methods are close. Most of the POW-I scatters are on the red line. Most of the POW-R scatters are close to the red line, and the errors are acceptable for most dips.

Table III shows the statistical data for the comparison, and the errors of difference sets (in proportion) are listed. The error exceeds  $90^\circ$  in 28 (6.6%) and 29 cases (8.2%) for POW-I and POW-R, respectively. The errors are less than  $20^\circ$  in 373 (87.8%) and 284 cases (80.5%) for POW-I and POW-R, respectively. The sampling frequency of the measured voltage dips is 96 samples/cycle, and one sample corresponds to about  $3.75^\circ$ . The deviation of  $20^\circ$  means about 5 sample points, which is still a small error.

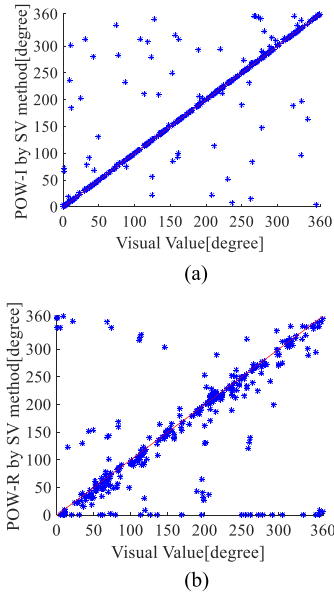


Fig. 12. POW by SV method versus Visual value. (a) Comparison of POW-I results. (b) Comparison of POW-R results.

TABLE III  
THE RESULTS OF DIFFERENT DEVIATIONS (BY SV METHOD)

Error	0-20°	20-40°	40-60°	60-90°	>90°
<b>POW-I</b>	373(87.8%)	5(1.1%)	4(0.9%)	15(3.5%)	28(6.6%)
<b>POW-R</b>	284(80.5%)	19(5.4%)	5(1.4%)	16(4.5%)	29(8.2%)

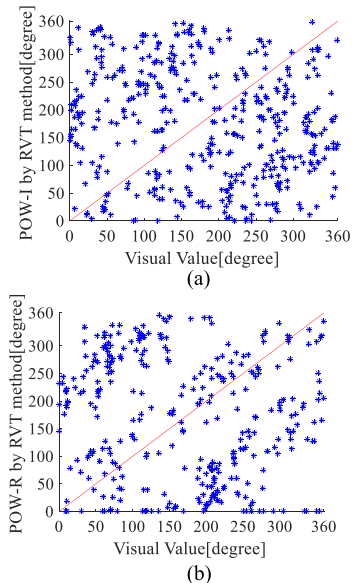


Fig. 13. POW by RVT method versus Visual value. (a) Comparison of POW-I results. (b) Comparison of POW-R results.

### C. Results by RVT & Visual Value

A comparison between the results by RVT method and Visual value, is shown in Fig. 13. The x-axis is Visual value, and y-axis is the result by RVT.

TABLE IV  
THE RESULTS OF DIFFERENT DEVIATIONS (BY RVT METHOD)

Error	0-20°	20-40°	40-60°	60-90°	>90°
<b>POW-I</b>	24(5.6%)	36(8.5%)	51(12%)	57(13.4%)	257(60.5%)
<b>POW-R</b>	36(10.2%)	37(10.5%)	27(7.6%)	25(7.1%)	228(64.6%)

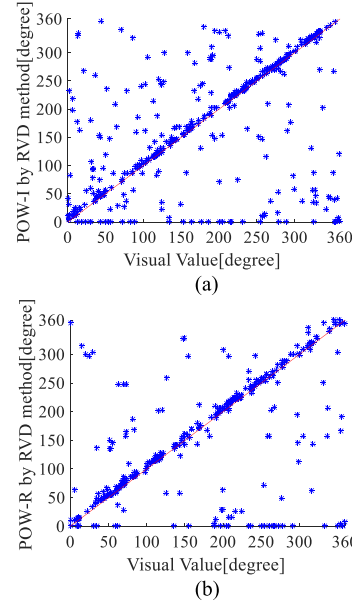


Fig. 14. POW by RVD method versus Visual value. (a) Comparison of POW-I results. (b) Comparison of POW-R results.

TABLE V  
THE RESULTS OF DIFFERENT DEVIATIONS (BY RVD METHOD)

Error	0-20°	20-40°	40-60°	60-90°	>90°
<b>POW-I</b>	279(65.6%)	19(4.5%)	27(6.4%)	31(7.3%)	69(16.2%)
<b>POW-R</b>	261(73.9%)	12(3.4%)	8(2.3%)	23(6.5%)	49(13.9%)

For POW-I or POW-R, there are only a few scatters close to the red line. Table IV shows the statistical data of the comparison, and the number of differences (in proportion) are listed. The error exceeds 90° in 257 cases (60.5%) and 228 cases (64.6%) for POW-I and POW-R, respectively.

From the theoretical analysis and the comparison of results, RVT cannot calculate POW accurately.

### D. Results by RVD & Visual Value

A comparison between the results by RVD method proposed in [15] and Visual value is shown in Fig. 14. Table V shows the statistical results, and the errors of difference (in proportion) are listed. The error exceeds 90° in 69 cases (16.2%) and 49 cases (13.9%) for POW-I and POW-R, respectively. The error is less than 20° in 279 cases (56.6%) and 261 cases (73.9%) for POW-I and POW-R, respectively.

For calculating both POW-I and POW-R, the accuracy of SV method is higher than of RVD. Moreover, the number of cases with error exceeding 90° by RVD, is greater than for

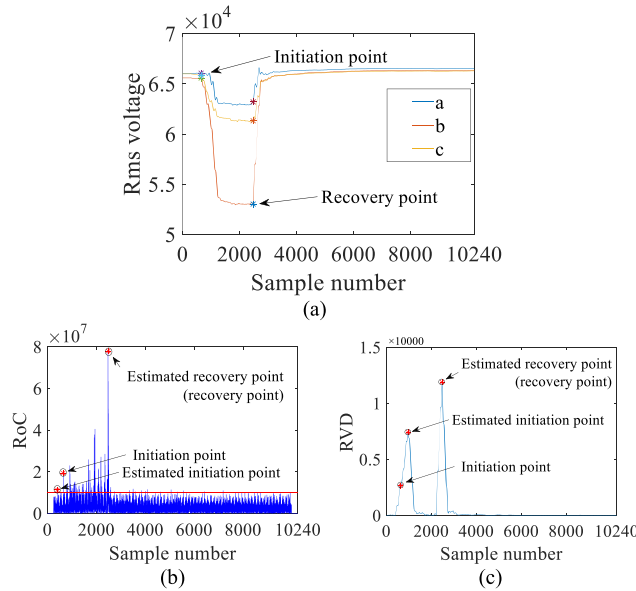


Fig. 15. Case study to explore the influence factors. (a) RMS voltage waveform. (b) Detection by SV method. (c) Detection by RVD method.

SV. It is concluded here that the proposed method has a better performance than the RVD method.

#### E. Case Study for SV & RVD

From the analysis mentioned above, the accuracy rate is different for SV method and RVD method, and there are cases where both methods get the wrong estimated results. An example (the sampling rate is 256 points/cycle) is shown in Fig. 15(a) to study what influences the performance of the methods.

The initiation point is 657th point and the recovery point is 2480th point in (a), by visual inspection. Correspondingly, POW-I is  $327.6563^\circ$ , and POW-R is  $11.2500^\circ$ .

By SV method, the estimated initiation point is sample 459, and the estimated recovery point is sample 2480, as shown in Fig. 15(b). It means the estimated POW-I is  $49.2188^\circ$ , and the estimated POW-R is  $11.2500^\circ$ . The initiation point has a greater error, possibly impacted by noise in this case. The noise in Fig. 15(b) shows similar features as in Fig. 10(b), which leads to an inappropriate threshold and the wrong result.

Applying the RVD method to the same dip, the estimated initiation point is sample 970, and the estimated recovery point is sample 2481, as shown in Fig. 15(c). The estimated POW-I is  $46.4063^\circ$ , and the estimated POW-R is  $12.6563^\circ$ . The detection of the recovery point and POW-R is accurate. The detection of the initiation point shows a large error. The reason is that the first transition segment is long (more than one cycle) and the magnitude of this dip is low, leading to that the greatest RVD is in the middle of the first transition segment, which is detected as the initiation point. Failure to find the initiation point accurately means that the calculation of POW-I is inaccurate. Therefore, RVD is affected by the magnitude change. Complex dips may show a fluctuation or a sudden change in the first or second transition segment, that may influence the performance of RVD.

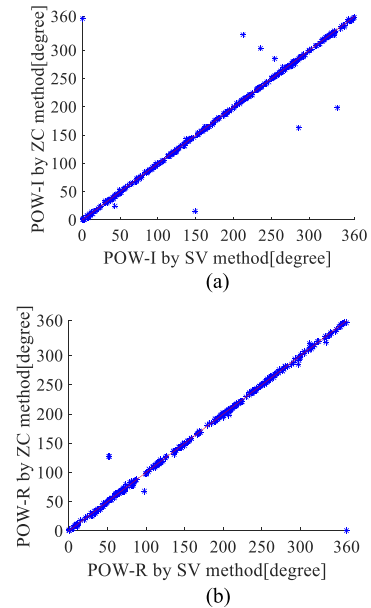


Fig. 16. POW by the proposed method versus by zero crossing method. (a) Comparison of POW-I results. (b) Comparison of POW-R results.

From the case study, it is clear that noise influences the performance of SV method, which is similar to the result from Section IV.G. However, the proposed threshold in this paper gives a good performance for the vast majority of cases. It is worth, as part of future work, to study the use of an adaptive threshold considering the influence of noise. Concerning the RVD method, POW is not the point with the highest RVD for complex voltage dips, like this example. Further study and improvement of the method is recommended.

#### F. Comparison of Angle Calculation Methods

For the existing methods [8], [23], a reference point is needed when calculating the angle of POW. “The upward zero crossing of the fundamental voltage is” such a reference point. This angle calculation method is called zero-crossing (ZC) method. In this paper, a new definition of POW is proposed based on SV. The angle of POW can be obtained directly by the angle between space vector and the real axis in the complex plane.

Theoretically, the POW obtained by SV is more accurate. The angle with reference to the upward zero crossing point is not a real “zero” point, due to the sampling and step size. Moreover, the algorithm for finding zero-crossing points may also be disturbed by noise.

Fig. 16 shows compares the results obtained by the two methods. Most of the results obtained by the two methods are consistent. In a few cases, the ZC method cannot find the correct zero-crossing point, which leads to errors in angle. Because of space limit, no more examples are given to analyze the errors of ZC method. Considering that the amount of computation of the SV method proposed in this paper is much less than that of ZC method, this paper recommends to use the proposed method to calculate the angle of POW.

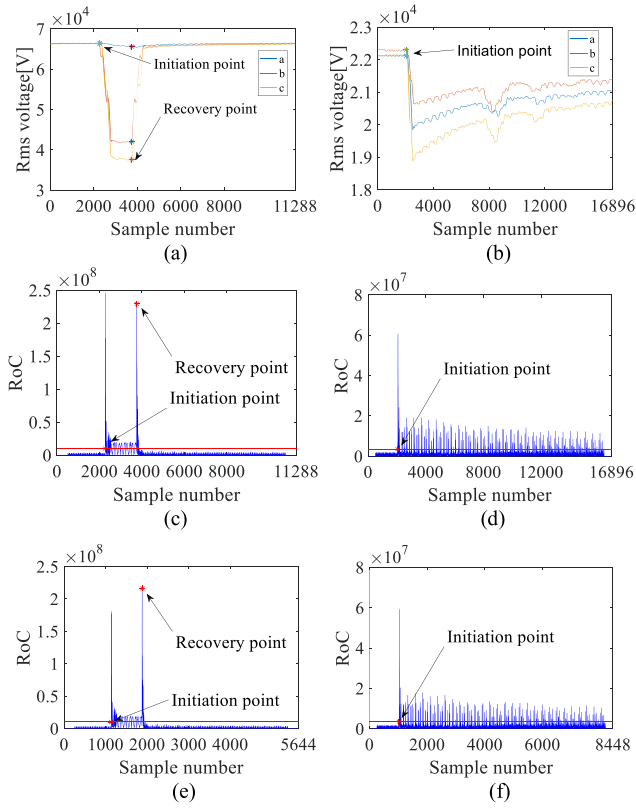


Fig. 17. Effect of the sampling rate. (a) RMS voltage of Example 4. (b) RMS voltage of Example 5. (c)  $RoC$  of Example 4 (512 sampling points/cycle). (d)  $RoC$  of Example 5 (512 sampling points/cycle). (e)  $RoC$  of Example 4 (256 sampling points/cycle). (f)  $RoC$  of Example 5 (256 sampling points/cycle).

TABLE VI  
THE EFFECT BY SAMPLING RATE FOR SV METHOD

Sampling points /cycle	Example 4			Example 5		
	POW-I		POW-R		POW-I	
	Sampling Number	Time (Cycle)	Sampling Number	Time (Cycle)	Sampling Number	Time (Cycle)
512	2273	4.44	3759	7.34	2058	4.02
256	1137	4.44	1880	7.34	1031	4.02
128	569	4.44	940	7.34	518	4.04
64	285	4.44	470	7.34	259	4.04

### G. Effect of the Sampling Rate

This paper reduces the sampling rate of two measured voltage dips, to study the effect of sampling rate on the performance of the proposed method. Two voltage dips are considered, including one unbalanced rectangular voltage dip (Example 4) and one unbalanced slowly recovering voltage dip (Example 5). The original sampling rate, 512 points/cycle, is reduced to 256/128/64 points/cycle (removed one point every other sampling point), to generate 3\*2 sets of voltage dips. The calculation results by the proposed method are shown in Fig. 17 and Table VI. The rms voltages of the two dips are shown in (a) and (b),  $RoCs$  of two dips with the sampling rate of 512 sampling points/cycle are shown in (c) and (d), and  $RoCs$  of the two dips with the sampling rate of 256 sampling points/cycle are in (e) and (f). The other  $RoC$  waveforms are not shown for limited space.

By visual inspection, get the information of Example 4 in Fig. 17(a). The initiation point and recovery point are sample 2273 and 3759, which are at 4.44 cycle and 7.34 cycle, respectively. Fig. 17(c) shows the detection result according to  $RoC$ , where the estimated results are consistent with the results of visual inspection when the sampling rate remains unchanged. Fig. 17(e) and Table VI show the estimated results when the sampling rate is reduced to 256/128/64 sampling points/cycle, the detected points have a different sampling number because of the different sampling rate. However, POW-I and POW-R are detected accurately at 4.44 and 7.34 cycles.

For Example 5 in Fig. 17(b), the initiation is at sample 2058, at 4.02 cycle, by visual inspection. Fig. 17(d) shows the estimated result by  $RoC$  for the original sampling rate. It is the same as the result by visual inspection. Fig. 17(f) and Table VI show the estimated results by the proposed method with reduced sampling rate to 256/128/64 points/cycle. The estimated results show that the proposed method has the good performance even for 64 sampling points /cycle.

In principle, the sampling rate does not have effect on the performance of the proposed method (except in extreme cases where the sampling rate is too low, there may be no method available to detect POW accurately in that case). When the sampling rate increases, the denominator  $\Delta t$  in (8) decreases, and the molecule  $|r(i)-r(i+1)|$  decreases too, which may not impact the  $RoC$  significantly. The same holds when the sampling rate decreases. The rate of change does not show a major change, when the sampling rate changes. To detect POW according to  $RoC$  is to detect the abrupt changing point. A tiny error due to a low sampling rate is possible, but there will not be a significant error. The comparisons between (c) and (e), between (d) and (f), show the abrupt changing point.

### H. POW Statistics Distribution

The statistical distribution of the POW values detected by the proposed method for the 425 voltage dips is shown in Fig. 18.

For POW-I, it is assumed that faults due to the insulation breakdown and the flashover are more likely to occur near voltage maximum or minimum theoretically. Thus POW-I may be at the instant that voltage is close to its maximum or minimum value [8], corresponding to POW-I of  $90^\circ$  or  $270^\circ$ . Fig. 18(a) for the 425 dips shows a similar distribution, POW-I values in the range of  $60^\circ$  -  $120^\circ$  and  $240^\circ$  -  $300^\circ$  form 54.82% of the total. There are 72 sets of voltage dips which are not due to fault, thus it is reasonable that POW-Is of those cases are out of the range.

For POW-R, the duration of dips due to a short circuit depends on the relay setting of fault clearing [32]. The circuit breaker clears the fault at current zero crossing, which means that the possible POW-R is close to  $90^\circ$  or  $270^\circ$ , corresponding to  $0^\circ$  or  $180^\circ$  for the current if current lags voltage by  $90^\circ$ . Assume X/R of source impedance at fault location is 2 or higher. All dips were measured at MV level, so that seems a reasonable assumption. That means current lags voltage by  $60^\circ$ - $90^\circ$  and most of POW-R should be in the range of  $60^\circ$ - $90^\circ$  or  $240^\circ$ - $270^\circ$ . Fig. 18(b) shows the distribution of POW-R, which is mainly

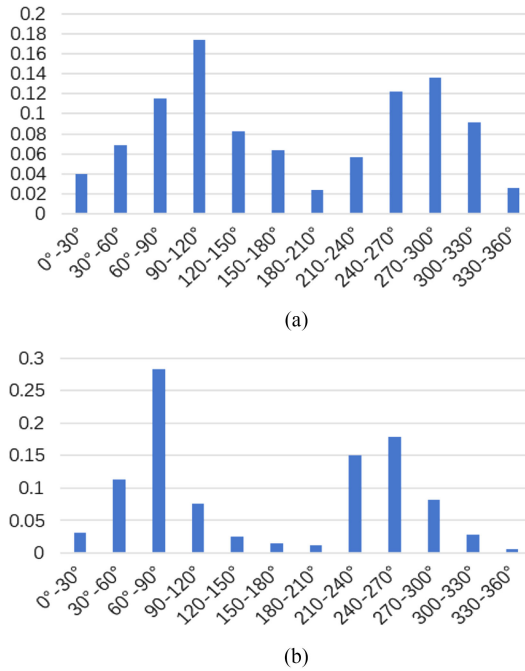


Fig. 18. Distribution of POW for the measured voltage dips. (a) Distribution of POW-I. (b) Distribution of POW-R.

distributed in 60°–90° and 240°–270°. POW-R values in the range of 60°–90° and 240°–270° form 46.18% among the total.

The results for POW-R show a clustering near 90° and 270°, as expected. However, the total number of cases in this range seems less than expected, which is explicable. For an unbalanced dip, the POW as a single-event is the POW of the phase with the lowest residual voltage. The measured waveform may be not in the voltage level of the fault location, but recorded at the other voltage level after propagation through a transformer, which may lead to the change of the dip type.

Fig. 18 shows the POW distribution of 425 measured voltage dip. The distribution proves the accuracy of the definition and the calculation method of the proposed method.

## VI. CONCLUSION

The definition and calculation of POW of voltage dips are unsolved issues in the field of power quality. This paper proposes a definition of POW for three-phase voltage dips, and a calculation method based on space vector, including POW detection and angle calculation. The performance and accuracy of the proposed method is verified using simulated voltage dips and 425 measured voltage dips, by comparing the method with published methods.

The conclusions of this paper can be summarized as follows:

- Due to the incompleteness of existing definitions, this paper presents a definition of POW for three-phase voltage dip. The POW distribution of 425 sets of measured voltage dips proves the rationality of the definition.
- The definition of POW for slowly recovering dips and multistage voltage dips are presented in this paper.

- The existing POW detection methods do not have a high accuracy. Therefore, based on space vector, this paper proposes an alternative detection and calculation method for POW.
- A simulation model of the power system has been built to generate dips due to short-circuit faults, motor starting, transformer energizing, simultaneous faults, and multi-stage faults. Dips with background harmonics and noise are considered as well. For all types of dips, even in the environment with very serious harmonic and noise, the proposed method shows a good performance.
- The detection of the proposed method for 425 measured voltage dip shows a good performance. 87.8% of 425 cases (for POW-I) and 80.5% of 353 cases (for POW-R) have an error less than 20°, compared with Visual value, respectively. Compared with the existing methods, the proposed method has a much better performance.
- The angle calculation method proposed in this paper is more accurate than the zero-crossing method. Moreover, the computational complexity of the proposed angle calculation method is less than that of the traditional zero-crossing method. Therefore, this paper recommends using the proposed method to calculate the angle of POW.
- Through the analysis of two measured voltage dips, it is shown that the proposed algorithm will not be affected by a reduced sampling rate.

## ACKNOWLEDGMENT

The main measurement data were obtained from State grid electric power research institute of Henan Electric power company, Göteborg Energi and Scottish Power.

## REFERENCES

- [1] IEC Electromagnetic Compatibility: Environment – Voltage Dips and Short Interruptions on Public Electric Power Supply Systems With Statistical Measurement, IEC 61000-2-8, 2000.
- [2] IEC Electromagnetic Compatibility: Testing and Measurements Techniques – Power Quality Measurement Methods, IEC 61000-4-30, 2015.
- [3] IEEE Recommended Practice for Monitoring Electric Power Quality, IEEE Std. 1159-2009, Jun. 2009.
- [4] M. H. J. Bollen, D. D. Sabin, and R. S. Thallam, “Voltage-sag indices – recent developments in IEEE P1564 task force,” in Proc. CIGRE/IEEE PES Int. Symp. Quality Secur. Electric Power Del. Syst., Oct. 2003, pp. 34–41.
- [5] IEEE Recommended Practice for Evaluating Electric Power System Compatibility with Electronic Process Equipment, IEEE Std. 1346-1998, May 1998.
- [6] EPRI the Effects of Point-on-Wave on Low-Voltage Tolerance of Industrial Process Devices, EPRI Brief 44, 1998.
- [7] EPRI Performance of a Hold-in Device for Relays, Contactors and Motor Starters, EPRI Brief 46, 1998.
- [8] S. Djokic, J. Milanovic, and S. Rowland, “Advanced voltage sag characterization II: Point-on-wave,” IET Gener. Transmiss. Distrib., vol. 1, no. 1, pp. 146–154, Jan. 2007.
- [9] S. M. Akolkar and B. E. Kushare, “Effect of point on wave angle on sensitivity of AC coil contactor and SMPS to voltage sags,” in Proc. Conf. IPEC, Oct. 2010, pp. 957–961.
- [10] S. Z. Djokic, J. V. Milanovic, and D. S. Kirschen, “Sensitivity of AC coil contactors to voltage sags, short interruptions, and undervoltage transients,” IEEE Trans. Power Del., vol. 19, no. 3, pp. 1299–1307, Jul. 2004.
- [11] S. Ouyang *et al.*, “Test and analysis on sensitivity of low-voltage releases to voltage sags,” IET Gener. Transmiss. Distrib., vol. 9, pp. 2664–2671, Nov. 2015.

- [12] J. Lopez *et al.*, "Wind turbines based on doubly fed induction generator under asymmetrical voltage dips," *IEEE Trans. Energy Convers.*, vol. 23, no. 1, pp. 321–330, Mar. 2008.
- [13] C. Chen *et al.*, "The impact of voltage dips to low-voltage-ride-through capacity of doubly fed induction generator based wind turbine," in *Proc. IEEE Milan PowerTech*, Jun. 2019, pp. 1–6.
- [14] Y. Wang, X. Y. Xiao, and M. H. J. Bollen, "Challenges in the calculation methods of point-on-wave characteristics for voltage dips," in *Proc. ICHQP*, Oct. 2016, pp. 513–517.
- [15] Power quality event characterization (1159.2). 2009. [Online]. Available: <http://group.ieee.org/groups/1159/2/>
- [16] *IEEE Guide for Voltage Sag Indices*, *IEEE Std. 1564-2014*, Mar. 2014.
- [17] F. B. Alvaro, W. L. Keng, T. Grazia, and S. Surya, "Accurate identification of point-on-wave inception and recovery instants of voltage sags and swells," *IEEE Trans. Power Del.*, vol. 34, no. 4, pp. 551–560, Apr. 2019.
- [18] A. C. Parsons, W. M. Grady, and E. J. Powers, "A wavelet-based procedure for automatically determining the beginning and end of transmission system voltage sags," in *Proc. IEEE Power Eng. Soc. Winter Meet.*, Feb. 1999, pp. 1310–1315.
- [19] E. Perez and J. Barros, "A proposal for on-line detection and classification of voltage events in power systems," *IEEE Trans. Power Del.*, vol. 23, no. 4, pp. 2132–2138, Oct. 2008.
- [20] F. Costa and J. Driesen, "Assessment of voltage sag indices based on scaling and wavelet coefficient energy analysis," *IEEE Trans. Power Del.*, vol. 28, no. 1, pp. 336–346, Jan. 2013.
- [21] O. Gencen, S. Ozturk, and T. Erfidan, "A new approach to voltage sag detection based on wavelet transform," *Int. J. Elect. Power Energy Syst.*, vol. 32, no. 2, pp. 133–140, Feb. 2010.
- [22] M. Latran and A. Teke, "A novel wavelet transform based voltage sag/swell detection algorithm," *Int. J. Elect. Power Energy Syst.*, vol. 71, pp. 131–139, Oct. 2015.
- [23] M. H. J. Bollen, *Understanding Power Quality Problem: Voltage Sag and Interruption*, Piscataway, NJ, USA: IEEE Press, 2000.
- [24] A. F. Bastos, S. Santoso, and G. Todeschini, "Comparison of methods for determining inception and recovery points of voltage variation events," in *Proc. IEEE Power Energy Soc. Gen. Meeting*, Aug. 2018, pp. 1–5.
- [25] V. Ignatova, P. Granjon, and S. Bacha, "Space vector method for voltage dips and swells analysis," *IEEE Trans. Power Del.*, vol. 24, no. 4, pp. 2054–2061, Oct. 2009.
- [26] E. Styvaktakis, M. H. J. Bollen, and I. Y. H. Gu, "Automatic classification of power system events using RMS voltage measurements," in *Proc. Power Eng. Soc. Summer Meet.*, Jul. 2002, pp. 824–829.
- [27] E. Styvaktakis and M. H. J. Bollen, "Signatures of voltage dip: Transformer saturation and multistage dips," *IEEE Trans. Power Del.*, vol. 18, no. 1, pp. 265–270, Jan. 2003.
- [28] A. Bagheri, M. H. J. Bollen, and I. Y. H. Gu, "Improved characterization of multi-stage voltage dips based on the space phasor model," *Electric Power Syst. Res.*, vol. 154, pp. 319–328, Jan. 2018.
- [29] J. R. Camarillo and G. Ramos, "Fault classification and voltage sag parameter computation using voltage ellipses," *IEEE Trans. Ind. Appl.*, vol. 55, no. 1, pp. 92–97, Jan./Feb. 2019.
- [30] J. R. Camarillo and G. Ramos, "Fault classification and voltage sag parameter computation using voltage ellipses," in *Proc. 54th Ind. Commercial Power Syst. Technol. Conf.*, May 2018, pp. 1–6.
- [31] *IEEE Recommended Practice and Requirements for Harmonic Control in Electric Power Systems*, *IEEE Std. 519-2014 (Revision of IEEE Std. 519-1992)*, 2014.
- [32] S. Hanninen *et al.*, "Characteristics of earth faults in power systems with a compensated or an unearthed neutral," in *Proc. 14th Int. Conf. Exhib. Electricity Distrib. Part 1. Contributions*, Jun. 1997, vol. 2, pp. 16/1–16/5.

**Ying Wang** (M'16–SM'17) received the B.S., M.S., and Ph.D. degrees from Sichuan University, Chengdu, China, in 2004, 2007, and 2014, respectively. During her Ph.D. studying, she had been a Visiting Student in electric power engineering with the Luleå University of Technology, Skellefteå, Sweden. She is currently an Associate Professor with Sichuan University. Her main research interests are in the area of voltage dips.

**Ling-Feng Deng** is currently a student with Sichuan University, Chengdu, China. His main research interests are in the area of voltage dip.

**Math H. J. Bollen** (M'93–SM'96–F'05) received the M.Sc. and Ph.D. degrees from the Eindhoven University of Technology, Eindhoven, The Netherlands, in 1985 and 1989, respectively. He is currently a Professor in electric power engineering with the Luleå University of Technology, Skellefteå, Sweden and R&D Manager Electric Power Systems with STRI AB, Gothenburg, Sweden. He has among others been a Lecturer with the University of Manchester Institute of Science and Technology, Manchester, U.K., a Professor in electric power systems with the Chalmers University of Technology, Gothenburg, Sweden, and a Technical Experts with the Energy Markets Inspectorate, Eskilstuna, Sweden. He has authored or coauthored a few hundred papers including a number of fundamental papers on voltage dip analysis, two textbooks on power quality, *Understanding Power Quality Problems* and *Signal Processing of Power Quality Disturbances*, and two textbooks on the future power system: *Integration of Distributed Generation in the Power System* and *The Smart Grid – Adapting the Power System to New Challenges*.

**Xian-Yong Xiao** (M'07–SM'16) received the Ph.D. degree from Sichuan University, Chengdu, China, in 2010. He is currently a Professor and Dean with the College of Electrical Engineering and Information Technology, Sichuan University. His research interests include power quality and its control, distribution system reliability, and green friendly smart grid.